Development of 154/116 GHz Dual-Frequency Gyrotron for the Large Helical Device

Tsuyoshi KARIYA[1)]*, Ryutaro MINAMI[1)], Takashi SHIMOZUMA[2)], Satoshi ITO[3)], Shin KUBO[4)], Hiroe IGAMI[2)], Masaki NISHIURA[2)], Mizuki SAKAMOTO[1)]

[1)] *Plasma Research Center, University of Tsukuba, Ibaraki 305-8577, Japan*
[2)] *National Institute for Fusion Science, National Institutes of Natural Sciences, Gifu 509-5292, Japan*
[3)] *ITER Organization, Heating & Current Drive Division, Saint-Paul-lez-Durance, France*
[4)] *College of Science and Engineering, Chubu University, Aichi 487-8501, Japan*

(Received 24 December 2024 / Accepted 28 January 2025)

Based on the successful results of three 77 and two 154 GHz gyrotrons development and their contributions to large helical device (LHD) plasma experiments, a new 154/116 GHz dual-frequency gyrotron was developed. The optimal combination of cavity oscillation modes for dual-frequency oscillations at 154 and 116 GHz and optimal designs for the electron gun, cavity, mode converter, RF transmission mirrors, output window, and collector were determined. In an experimental test of the 154/116 GHz dual-frequency gyrotron, maximum powers of 1.66 and 1.34 MW were achieved at 154.05 and 116.15 GHz with pulse widths of 2.5 ms, respectively.

Keywords: gyrotron, dual-frequency, MW, ECRH, LHD

DOI: 10.1585/pfr.20.1402022

1. Introduction

Gyrotrons are powerful tools for the electron cyclotron heating (ECH), electron cyclotron current drive (ECCD), and electron Bernstein wave (EBW) heating. Each fusion experimental device requires an optimal gyrotron with a frequency suitable for the magnetic field strength and experimental method. Although the frequency of the gyrotron cannot be varied continuously, gyrotrons capable of operateing discretely at two or three frequencies have recently been developed. In the 100 GHz range, dual- or multi-frequency MW gyrotrons are being developed at various facilities for nuclear fusion purposes [1–8].

A joint program between the National Institute for Fusion Science (NIFS) and University of Tsukuba developed three 77 and two 154 GHz gyrotrons for the Large Helical Device (LHD) [9–12]. Typically, 77 GHz gyrotrons achieved a maximum output power of 1.9 MW and quasi-CW 75-minute-long operation at 0.22 MW. The 154 GHz gyrotrons achieved a maximum output power of 1.25 MW and 30 min of operation at 0.35 MW. A total plasma-injection power of 5.4 MW was achieved using these gyrotrons.

Gyrotrons have enhanced LHD plasma performance in recent electron internal transport barrier (ITB) experiments [13]. High-temperature plasmas with simultaneously high electron (7–9 keV) and ion (4–6 keV) temperatures were obtained by combining high-power ECH and neutral beam injection (NBI) [14]. A steady-state plasma with a line-averaged electron density of 1×10^{19} m^{-3} and an electron temperature of 3.5 keV was sustained for 330 s [15].

As the next step in NIFS gyrotron development, a 154/116 GHz dual-frequency gyrotron was developed to expand the range of LHD plasma parameters [16]. It is feasible to increase the injection power at 154 GHz and the third-harmonic heating by 116 GHz. Effective third-harmonic heating is expected by injecting 116 GHz into a high-electron-temperature plasma heated by the 77 GHz second-harmonic. Additionally, the 116 GHz wave heating is expected to provide effective peripheral and EBW heating in super-dense core plasma (SDC).

The remainder of the paper is organized as follows. Sections 2 and 3 present the design and initial test results of the new 154/116 GHz dual-frequency gyrotron, respectively. A summary and conclusions are presented in Sec. 4.

2. Design of the 154/116 GHz Dual-Frequency Gyrotron

To determine the optimal combination of cavity oscillation modes, the frequencies of the main- and sub-mode were set to 154 and 115.5 ± 0.5 GHz, which is suitable for third harmonic heating, respectively. The design targets for output power were set at over 1 MW for 154 GHz and over 0.7 MW for 115.5 ± 0.5 GHz. The difference between the radiation angles of the mode converter for the 154 and 115.5 ± 0.5 GHz cavity modes had to be approximately 0° to achieve high

Corresponding author's e-mail: kariya@prc.tsukuba.ac.jp

radio frequency (RF) beam transmission efficiency for both modes using the same internal mirrors.

Additionally, under the magnetic field distribution produced by the superconducting magnet (SCM), a magnetron injection gun (MIG) was designed to inject the electron beam at the first peak of the cavity electric field for both oscillation modes with an electron beam pitch factor α = 1.0–1.2. The pitch factor α is defined as the ratio of the perpendicular velocity of the electron beam relative to the magnetic field to its parallel velocity. The frequency band of the output window was designed to match both frequencies. Based on these considerations, the combination of the cavity oscillation modes were determined as $TE_{28,9}$ and $TE_{21,7}$ at 154 and 116 GHz, respectively.

The calculated dependence of cavity oscillation power P_c and oscillation efficiency η_c on the beam current I_k at 154 and 116 GHz are shown in Figs. 1(a) and (b), respectively. The results indicate that higher values of α lead to greater η_c and P_c. For 154 and 116 GHz, oscillation powers above 1.5 and 1 MW, respectively, are expected with α = 1 (expected value in an actual MIG) for a beam voltage V_k = 80 kV, beam current I_k = 60 A and an electron beam radius R_e = 9.13 mm.

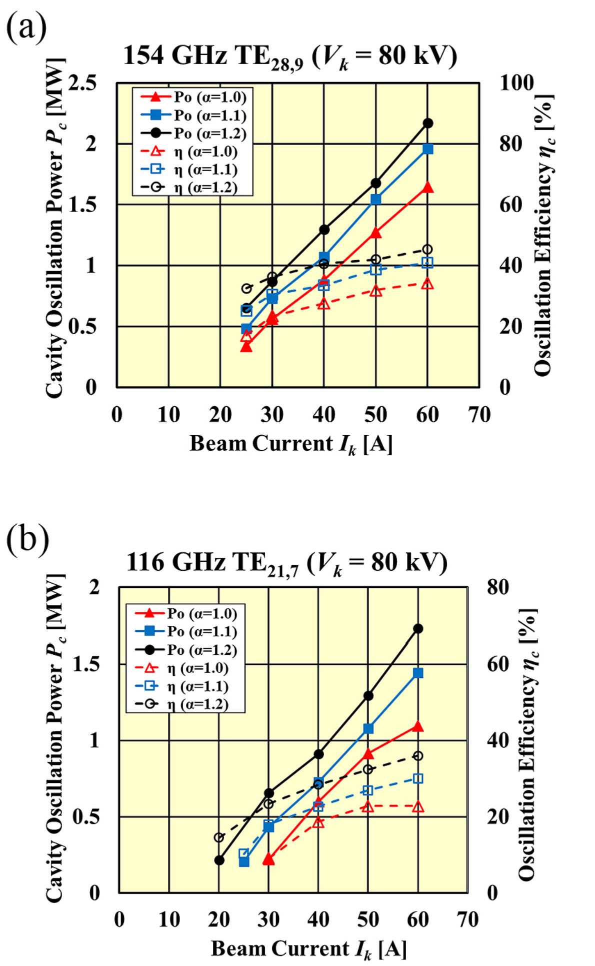

Fig. 1. Calculated dependence of the cavity oscillation power and oscillation efficiency on the beam current at (a) 154 and (b) 116 GHz for each pitch factor α of 1.0, 1.1 and 1.2.

The MIG is a triode gun that controls the electron beam parameters through the anode voltage. It has the same cathode structure as the 77 GHz #3 and 154 GHz gyrotrons, which ensures compatibility. The dependence of the pitch factor α and its spread $\Delta\alpha/\alpha$ calculated on the anode voltage V_{ak} using the MIG simulation code specialized in the electron gun of gyrotrons is shown in Fig. 2. The MIG is expected to operate efficiently at both 154 and 116 GHz with α = 1–1.2 and $\Delta\alpha/\alpha$ < 5% at V_k = 80 kV and I_k = 60 A, indicating high-efficiency oscillations in the cavity.

An RF absorber composed of SiC ceramics was inserted into the beam tunnel to suppress parasitic oscillations.

The cavity oscillation $TE_{m,n}$ mode RF wave was converted into a Gaussian-like beam using a built-in quasi-optical mode converter, which was optimized for both the 154 GHz $TE_{28,9}$ and 116 GHz $TE_{21,7}$ modes using the electric field integral equation code SURF3D [17]. A system of four elliptical mirrors (without phase-correcting mirrors) was used to focus the RF beam radiating from the mode converter and transmit it outside the tube through the output window. The calculated RF beam at the output window exhibited a clear Gaussian beam profile at both 154 and 116 GHz. The total calculated transmission efficiencies at the output window were 97.8% and 98.1% at 154 and 116 GHz, respectively.

The output window was a CVD diamond window with an effective aperture diameter and thickness were 85 mm and 1.63 mm, respectively. The power reflectance of the diamond window was 0% and 0.2% at 154 and 116 GHz, respectively.

The collector incorporated a collector potential depression (CPD) mechanism to improve efficiency and utilizes sweep coils to reduce the heat load of the spent electron beam on the collector. The efficiency is enhanced by a factor of V_k/V_M, where the total efficiency with CPD is $\eta_{cpd} = \eta_o V_k/V_M$, where V_M (= $V_k - V_{cpd}$) and V_{cpd} are the main power supply and CPD voltages, respectively. V_{cpd} is the beam deceleration voltage supplied between the body section (including the beam tunnel, cavity, mode converter, and mirrors) and collector, while η_o is the output efficiency. The sweeping frequency was maintained at 1–2 Hz to reduce attenuation of the sweep magnetic field caused by eddy currents on the metal surface

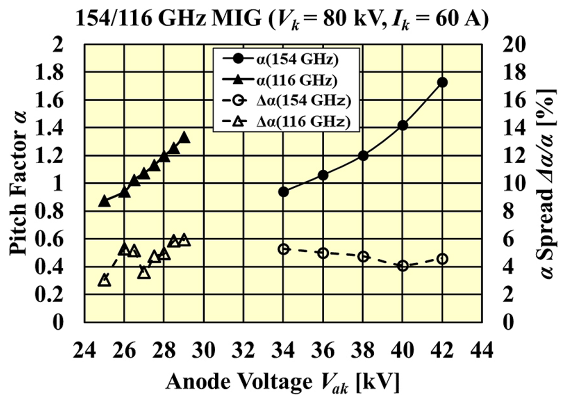

Fig. 2. Anode voltage dependencies of α and $\Delta\alpha/\alpha$ for MIG operations at 154 and 116 GHz.

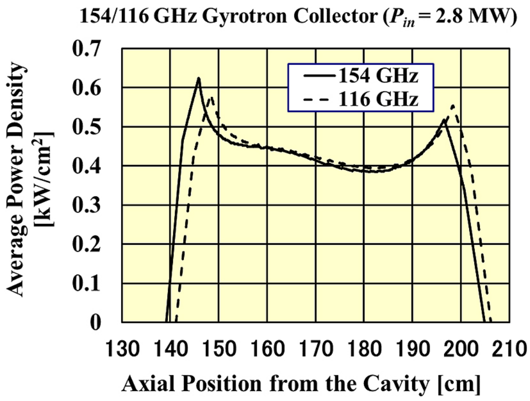

Fig. 3. Axial distribution of the heat load of the 2.8 MW spent beam on the collector for 154 and 116 GHz.

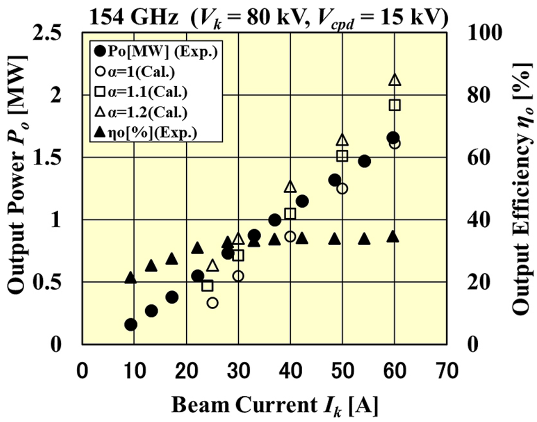

Fig. 4. Dependence of the experimental and calculated output power on the beam current at 154 GHz including experimentally obtained output efficiencies.

of the collector. The axial distributions of the average deposition power density on the collector (inner diameter: 320 mm) are shown in Fig. 3. The peak average deposition power densities for both frequencies are lower 0.6 kW/cm^2 with a spent beam power of 2.8 MW. This deposition power density was at the same level as that of the ITER 170 GHz gyrotron. These results indicate that the collector can operate at 1 MW in continuous (CW) mode.

3. Performance Test of the 154/116 GHz Dual-Frequency Gyrotron

An initial short-pulse test was performed using the NIFS power supply. The dependences of the experimentally obtained window output power (●) and output efficiency (▲) on the beam current I_k at 154 and 116 GHz are shown in Figs. 4 and 5, respectively. The output efficiencies excluded the CPD enhancement factor. Gaussian-like beam outputs of 1.66 MW with an efficiency of 34.8% at 154.05 GHz (Fig. 4) and 1.34 MW with an efficiency of 28.2% at 116.15 GHz (Fig. 5) were obtained. The measured RF oscillation pulse widths were 2.5 ms.

The calculated output powers for each electron beam pitch factor α are also plotted using open symbols in Figs. 4 and 5. The calculated output powers were adjusted based on the calculated cavity oscillation power at each α between 1.0 and 1.2 and the calculated transmission efficiency from the mode converter to the window. A comparison of the experimental and calculated results at 154 and 116 GHz revealed that α decreased at high I_k, with estimated values of 1–1.05. A high-power wave oscillation is generated based on the interaction between the vertical velocity of the electrons and the electromagnetic field in the cavity resonator. Typically, higher α is associated with higher oscillation efficiencies. However, if α increases significantly, the electrons are reflected by the mirror magnetic field formed by the SCM before entering the cavity. The current density, space charge effect, and influence of the non-uniformity of the emission belt surface increase with the electron beam current. The value of α varies depending on the spatially electron-emitting position

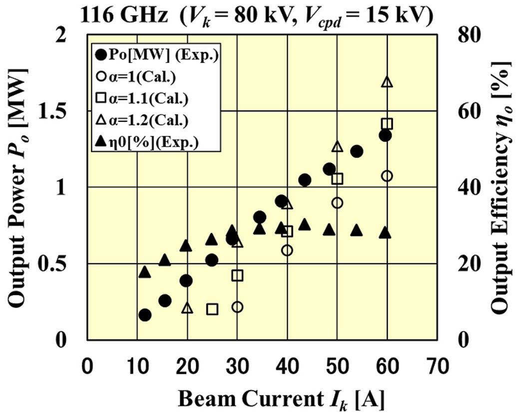

Fig. 5. Dependence of the experimental and calculated output power on the beam current at 116 GHz including experimentally obtained output efficiencies.

of the emission belt and is non-uniform throughout the electron beam. Additionally, the space charge effect reduces the voltage of the electron beam. These phenomena increase the anode current because of the reflected electrons and decrease the cavity oscillation efficiency. Thus, achieving large α values at high currents remains a challenge for the development of multi-MW gyrotrons.

The profile and phase of the window output RF beam were adjusted using a matching optics unit (MOU) and coupled to a corrugated waveguide in the HE_{11} mode. As shown in Figs. 6(a) and (b), the experimentally obtained transmission efficiencies of the MOU for coupling the window output to the corrugated waveguide were 96 ± 1% and 94 ± 1% at 154 and 116 GHz, respectively. The MOU transmission efficiencies were calculated by dividing the output efficiency at the MOU output (η_{mou}) by that at the window (η_o). The MOU transmission efficiency was measured on separate days before and after installing the MOU. For the same cathode heater power setting, I_k was not exactly the same. When the MOU was installed, the output power at the output window was different owing to variations in I_k reproducibility. Therefore, the MOU transmission efficiencies were calculated using

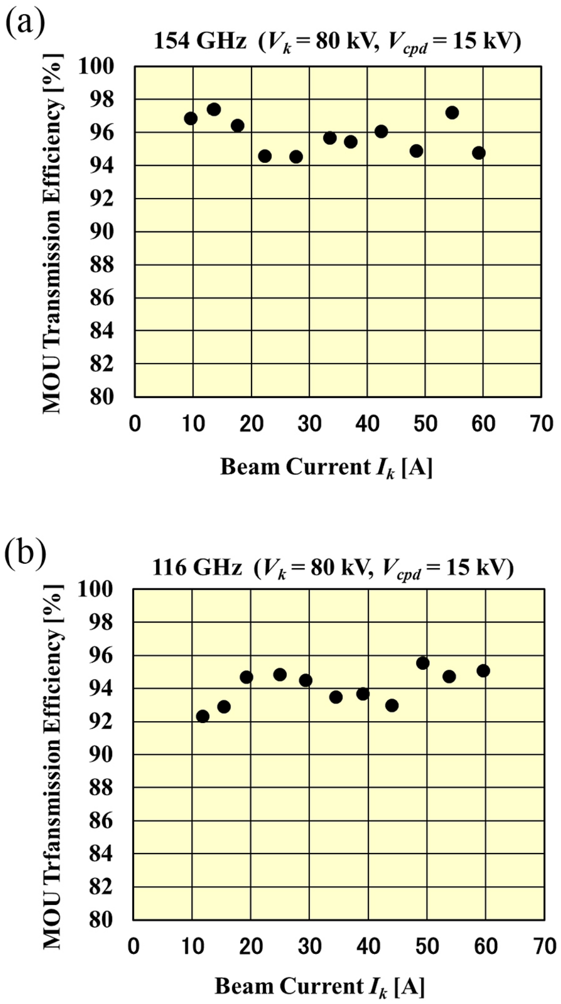

Fig. 6. Transmission efficiencies of the MOU for (a) 154 and (b) 116 GHz operations.

the output efficiency, which exhibited smaller changes than the output power for differences in I_k. By measuring the I_k dependence of η_{mou}/η_o and increasing the number of data points, the transmission efficiency of the MOU was statistically evaluated considering the variances of reproducibility and measurement error. The experimentally obtained values are consistent with the designed MOU transmission efficiencies of 97.3% and 94% at 154 and 116 GHz, respectively.

Long-pulse tests were performed using a long-pulse dummy load with V_k = 80 kV and V_{cpd} = 15 kV. An MOU output power of 1.16 MW (P_o = 1.21 MW, η_o = 34.2%, η_t = 42.2%, I_k = 44 A) at 154 GHz was achieved with a pulse width of 1 s. An MOU output power of 0.65 MW (P_o = 0.69 MW, η_o = 23.3%, η_t = 28.6%, and I_k = 37 A) at 116 GHz was achieved with a pulse width of 1 s. In long-pulse operation, the operating parameters must be adjusted compared to those of short-pulse tests because of the time evolution of the power supply voltage, gyrotron currents, and electron beam voltage [18].

This gyrotron was first used in LHD plasma experiments in 2021 and plasma injection powers of approximately 1 and 0.5 MW at 154 and 116 GHz, respectively, with a pulse widths of 2 s were achieved. In third-harmonic heating at 116 GHz in low-density plasma, a current driven by high energy electrons has been suggested. Upon high-power injection into the plasma, the gyrotron operation was sometimes influenced by the reflected power of the transmission system or plasma. The power and pulse width of the gyrotron were determined based on the requirements of the LHD experiments.

4. Summary and Conclusions

A new 154/116 GHz dual-frequency gyrotron was developed to increase the injection power at 154 GHz and perform third-harmonic heating by the 116 GHz. The optimal combination of cavity oscillation modes for dual-frequency oscillations were determined as $TE_{28,9}$ and $TE_{21,7}$ at 154 and 116 GHz, respectively, and optimal designs for the electron gun, cavity, mode converter, RF transmission mirrors, output window, and collector were obtained.

An experimental test of the 154/116 GHz dual-frequency gyrotron for LHD achieved maximum powers of 1.66 and 1.34 MW at 154.05 and 116.15 GHz with pulse widths of 2.5 ms, respectively. This gyrotron was successfully used in LHD plasma experiments to enhance the injection power at 154 GHz and perform third-harmonic heating at 116 GHz.

Acknowledgments

The authors thank the members of the NIFS ECRH group. This study was partially supported by the NIFS Collaborative Program (grant nos: COD28740, COD29746, COD30735, COD01736, and CKD02733).

[1] M. Thumm *et al.*, IEEE Trans. Plasma Sci. **35**, 143 (2007).
[2] D.S. Tax *et al.*, IEEE Trans. Plasma Sci. **42**, 1128 (2014).
[3] L. Diwei *et al.*, Fusion Eng. Des. **87**, 1533 (2012).
[4] A.G. Litvak *et al.*, Proc. 17th Joint Workshop on ECE and ECRH (EC-17) EPJ Web 32, 04003 (2012).
[5] S. Alberti *et al.*, EPJ Web of Conf. **157**, 03001 (2017).
[6] T. Kobayashi *et al.*, Trans. Fusion Sci. Technol. **63**, 160 (2013).
[7] K. Sakamoto *et al.*, Nucl. Fusion **49**, 095019 (2009).
[8] K. Sakamoto *et al.*, IEEE 14th International Vacuum Electronics Conf. Print ISBN: 978-1-4673-5976-4 (2013).
[9] T. Kariya *et al.*, Trans. Fusion Sci. Technol. **55**, 91 (2009).
[10] H. Takahashi *et al.*, Trans. Fusion Sci. Technol. **57**, 19 (2010).
[11] R. Minami *et al.*, Nucl. Fusion **53**, 063003 (2013).
[12] H. Takahashi *et al.*, Phys. Plasmas **21**, 061506 (2014).
[13] H. Igami *et al.*, EPJ Web of Conferences **203**, 02001 (2019).
[14] H. Takahashi *et al.*, Nucl. Fusion **57** 086029 (2017).
[15] Y. Yoshimura *et al.*, Plasma Phys. Control. Fusion **60** 025012 (2018).
[16] T. Kariya *et al.*, Nucl. Fusion **57**, 066001 (2017).
[17] J.M. Neilson and R. Bunger, IEEE Trans. Plasma Sci. **30**, 794 (2002).
[18] H. Takahashi *et al.*, Plasma Fusion Res. **7**, 1205154 (2012).